STABILITY OF PLANAR SHEAR FLOW IN THE PRESENCE OF ELECTROCONVECTION

Fulvio Martinelli
Laboratoire d'Hydrodynamique (LadHyx)
CNRS – École Polytechnique
F-91228 Palaiseau cedex – France
fulvio.martinelli@ladhyx.polytechnique.fr

Maurizio Quadrio
Dept. Aerospace Engineering
Politecnico di Milano
Campus Bovisa, Milano – Italy
maurizio.quadrio@polimi.it

Peter J. Schmid
Laboratoire d'Hydrodynamique (LadHyx)
CNRS – École Polytechnique
F-91228 Palaiseau cedex – France
peter@ladyhx.polytechnique.fr

ABSTRACT

The first complete study of linear, modal and non-modal stability of the EHD electroconvection problem with and without cross-flow is presented. Emphasis is put on understanding how electroconvection changes the stability characteristics of the plane Poiseuille flow.

INTRODUCTION

The present work concerns the field of electrohydrodynamics (EHD), which studies the action of an electric field upon *dielectric* fluids which, due to their low electrical conductivity, do not give rise to large electric currents, and hence render the effects of magnetic field negligible. EHD is thus the dual case of magneto-hydrodynamics (MHD) where conducting liquids with large electrical currents, negligible electric fields and strong magnetic fields prevail. In particular, in this work we address the so-called electroconvection problem. In the typical electroconvection problem, ions are injected into the bulk fluid from the boundary (typically by electrochemical reactions) under the action of an external electric field; only the Coulomb force is able to induce fluid motion, and the resulting mathematical problem is fully coupled, linking the well-known Navier-Stokes equations to the spatio-temporal evolution equation for the electric charge density. For suitable values of the electric forcing, large-scale rolls develop owing to an instability mechanism.

Several studies of electroconvection are available, dating back to the '70s and '80s and often motivated by a technological interest in Coulomb-driven convection (Felici, 1971; Crowley, 1986). Perhaps the most widespread interest and application arose from a desire to increase the heat transfer on large distribution power transformers, where lower temperatures yield increased efficiency; other applications with dielectric liquids, where injected ions represent the main source of charge, encompass those in electrostatic precipitators, EHD

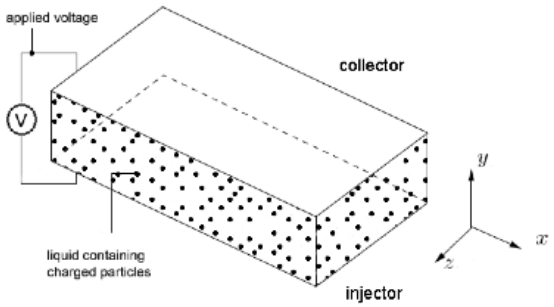

Figure 1. Sketch of the geometry (considered in the present work) and the coordinate system. When present, the cross-flow is directed along the *x* (streamwise) direction.

ion-drag pumps, EHD turbulent mixers. Applications containing liquid crystals or industrial processes involving metal casting have also prompted research into EHD. More recently, with the thriving boom in micro- and nano-fluid dynamical applications, interest of EHD flows is rising rapidly, mostly based on its potential for increasing mixing and heat transfer in micro- or nano-devices.

Most studies available in the literature contain simple configurations, like the cylindrical geometry or the planar one depicted in figure 1, where two solid walls (the injector and the collector) are present, across which a difference of electric potential is established to inject ions from one wall into the fluid and with the interior space filled by a dielectric fluid containing charged particles. For low-voltage forcing, the inherent viscous damping of the system is sufficient to ensure a stable motion, while at higher forcing levels the fluid is set into motion characterized by large-scale rolls. This stability problem resembles that of Rayleigh-Bénard convection, where the

temperature plays the analogous role to that of the charge density and the heat flux on the high-temperature wall acts as the forcing analogous to the potential difference in electroconvection. As soon as the instability sets in, however, macroscopic phenomena in EHD appear (such as the segregation of charge, i.e. the creation of large regions virtually free of charge) which have no counterpart in Rayleigh-Bénard.

The asymptotic stability of small perturbations to the electroconvective flow has been studied, both experimentally and numerically, over the last three decades, with two reviews by Castellanos (1991) and Atten (1996). To date, however, the critical value of the forcing parameter above which instability sets in remains a subject of some controversy, with numerical analyses predicting values about 50% higher than experimental investigations (Castellanos, 1991). On the other hand, the stability of wall-bounded shear flows of dielectric liquids in the presence of charge injection has received considerably less or no attention at all, and we are only aware of one single paper (Castellanos & Agrait, 1992) on the subject. In that paper, moreover, only weak ion injection is considered, and the two-way coupling between the velocity and electric fields is neglected. Furthermore, EHD (with or without cross-flow) has never been studied from the viewpoint of non-modal stability, to ascertain (or refute) whether transient growth mechanisms are at play (Schmid & Henningson, 2001).

We thus set as our long-term goal to understand how EHD effects can modify a shear flow, for example, plane Poiseuille flow, in the laminar, transitional and fully turbulent regime. The large-scale convective cells associated with the electroconvective instability make this kind of electric forcing a potential and attractive candidate for effectively creating large-scale vortical structures in a shear flow, especially considering its almost negligible power requirements. Such vortices might be exploited as flow control actuators leading, for example, to reduced friction drag (Schoppa & Hussain, 1998) or to substantial changes in heat transfer efficiency. The goal of the present paper is thus to present an initial stability study of EHD flow with and without (laminar) cross flow, performing both modal and non-modal analyses. It is worth noting that, for the first time, we will consider finite values of charge diffusivity, and this decision will be shown to bring about important consequences. Finally we will assess, though still in a preliminary way, the idea of exploiting EHD instabilities to create large-scale vortical structures that may be used in flow-control applications.

PROBLEM DEFINITION

We consider the planar geometry sketched in figure 1, where the used coordinate system is also introduced. The x direction is the streamwise direction of the laminar Poiseuille flow, when such a cross-flow is considered. The flow is governed by the incompressible Navier-Stokes equations, augmented by an electric force $\mathbf{F}_q/\rho$ that acts as a body force per unit mass. The electric force, in turn, satisfies a constitutive equation that, under the quasi-electrostatic limit, simplifies to an expression involving only the Coulomb force. Neglecting dielectric and electro-strictive forces one obtains

$$\frac{\mathbf{F}_q}{\rho} = q\mathbf{E} = \frac{\varepsilon}{\rho}\nabla^2\Phi\nabla\Phi. \qquad (1)$$

where q is the charge density, $\mathbf{E} = -\nabla\Phi$ is the electric field and Φ is the electric potential. Gauss' law $\nabla^2\Phi = -q/\varepsilon$ links the electric potential and the charge density (with ε as the fluid permittivity, assumed uniform).

The conservation law for q involves the divergence of its flux vector $\mathbf{J}$ which, in the present context, contains three contributions: convection of charge due to fluid motion, a drift induced by the external electric field beyond the zero-net random motions of the electrons, and diffusion. It can be written:

$$\mathbf{J} = q\mathbf{V} + qK\mathbf{E} - D\nabla q,$$

with K and D as the ionic mobility and charge diffusion coefficients. It can be observed that $K\mathbf{E}$ is the migration (drift) velocity of ions under action of the electric field. An evolution equation for the charge density is then formulated, and the equivalent fourth-order equation for Φ reads

$$\frac{\partial}{\partial t}\nabla^2\Phi + \nabla\cdot\left(\nabla^2\Phi\mathbf{V} - K\nabla^2\Phi\nabla\Phi + D\nabla^2(\nabla^2\Phi)\right) = 0. \quad (2)$$

The system consisting of the incompressible Navier-Stokes equations coupled via (1) to equation (2) has to be supplemented by a set of boundary conditions. Periodic conditions are employed in the homogeneous directions, while at the walls no-slip conditions are used for fluid velocities. At the walls, which are a distance $2h$ apart, the electric potential is set to $\Phi(h) = \Phi_0$ and $\Phi(-h) = 0$. The mechanism by which charge is injected at the wall at $y = -h$ (injector) and removed at the opposite wall (collector) remains to be specified. It is customary in the literature (Castellanos, 1991) to model this process under the assumption of autonomous (i.e. independent of the electric field) and unipolar (one single charge) injection, which implies a non-homogeneous Dirichlet boundary condition $q(-h) = q_0$ at the injector, and a homogeneous Neumann condition $\partial q/\partial y|_{y=h} = 0$ at the collector, i.e.,

$$\nabla^2\Phi|_{y=-h} = -q_0/\varepsilon; \qquad \frac{\partial}{\partial y}\nabla^2\Phi|_{y=h} = 0.$$

Numerical method

Before discretization, it is convenient to convert the governing equations to non-dimensional form. The problem is parametrized by four non-dimensional groups, built using h as the reference length, Φ_0 as the reference potential, $K\Phi_0/h$ as the reference velocity, $h^2/(K\Phi_0)$ as the reference time and $\rho K^2\Phi_0^2/h^2$ as the reference pressure. The four resulting parameters are (i) the charge injection coefficient $C = \frac{h^2 q_0}{\varepsilon\Phi_0}$, directly related to the boundary condition for the injection of charge, (ii) the Taylor parameter $T = \frac{\varepsilon\Phi_0}{\mu K}$, which expresses the ratio of the electric forcing of the system to its inherent viscous damping; (iii) the dimensionless charge diffusivity $Fe = \frac{K\Phi_0}{D}$, and, lastly, (iv) the dimensionless ionic mobility $M = \frac{1}{K}\sqrt{\varepsilon\rho}$.

After applying a Fourier transform along the homogeneous directions x and z, and linearizing about a a parabolic Poiseuille base flow $\overline{U}(y)$ and a base profile for $\overline{\Phi}$ (which can

be computed analytically), the resulting linearized equations for the perturbations read

$$\frac{\partial \hat{\Delta}\hat{v}}{\partial t} = -j\alpha\overline{U}\hat{\Delta}\hat{v} + j\alpha\overline{U}''\hat{v} + M^2\left[\overline{\Phi}'''\kappa^2\hat{\psi} - \overline{\Phi}'\kappa^2\hat{\Delta}\hat{\psi}\right] + \frac{M^2}{T}\hat{\Delta}\hat{\Delta}\hat{v}$$
$$\frac{\partial \hat{\eta}}{\partial t} = -j\beta\overline{U}'\hat{v} - j\alpha\overline{U}\hat{\eta} + \frac{M^2}{T}\hat{\Delta}\hat{\eta}$$
$$\frac{\partial \hat{\Delta}\hat{\psi}}{\partial t} = \overline{\Phi}'\frac{\partial \hat{\Delta}\hat{\psi}}{\partial y} + \overline{\Phi}'''\frac{\partial \hat{\psi}}{\partial y} + 2\overline{\Phi}''\hat{\Delta}\hat{\psi} - j\alpha\overline{U}\hat{\Delta}\hat{\psi} - \overline{\Phi}'''\hat{v} + \frac{1}{Fe}\hat{\Delta}\hat{\Delta}\hat{\psi},$$

where $\hat{v}$, $\hat{\eta}$ and $\hat{\psi}$ denote perturbations of the wall-normal velocity, wall-normal vorticity and potential. It is worth noticing that, with the present choice of velocity and length scales, the role usually played by the Reynolds number in plane Poiseuille flow is taken by the non-dimensional group T/M^2. With this in mind, one easily recovers the Orr-Sommerfeld-Squire equations in the normal velocity-normal vorticity formulation after setting $\overline{\Phi} = 0$. The composite parameter M contains fluid properties and geometric quantities and can thus be considered a material parameter; on the other hand, C, T and Fe contain both fluid and flow properties.

The governing equations are then spectrally discretized using N Chebyshev polynomials. The modal stability problem is equivalent to solving an eigenvalue problem and in particular to identifying the eigenvalue with the largest real part. The non-modal stability problem, in contrast, searches for short-time growth of the perturbation energy. In the hydrodynamic case, defining energy as the kinetic energy of the flow is an obvious choice. Here, choosing a physically sound norm to quantify the disturbance amplitude is key to obtaining meaningful results. We define our energy as the sum of a mechanical contribution (the kinetic energy of the flow) and an electrical contribution, i.e. $E_{tot} = E_{flow} + E_{\psi}$. The final expression, in $\hat{v} - \hat{\eta} - \hat{\Psi}$ form, reads

$$E_{tot} = \frac{1}{4}\sum_{\alpha,\beta}\int_{-1}^{1}\frac{1}{\kappa^2}\left(|\hat{\eta}|^2 + |\frac{d\hat{v}}{dy}|^2\right) + |\hat{v}|^2 + M^2\left(\kappa^2|\hat{\psi}|^2 + |\frac{d\hat{\psi}}{dy}|^2\right)dy.$$

THE HYDROSTATIC CASE (NO CROSS-FLOW)

We consider first the purely hydrostatic case, where electroconvection takes place in the absence of any pressure-gradient driven cross-flow.

Modal stability

Modal stability for this problem has already been addressed in the literature, but this is the first time, to our knowledge, that the effects of charge diffusion are accounted for. We first consider in figure 2 the neutral stability curves for different values of Fe. The critical value T_{cr} of the Taylor number is observed to vary significantly with Fe. The value $T_{cr} = 161$, present in the literature for the strong-injection regime (Castellanos, 1991) from studies neglecting diffusion, seems to be recovered in the limit $Fe \to \infty$, but non-zero diffusion appears to lower T_{cr} significantly, thus pointing to a destabilizing effect of charge diffusion. The wavenumber κ of the most unstable disturbance, on the other hand, does not appear to vary significantly with Fe.

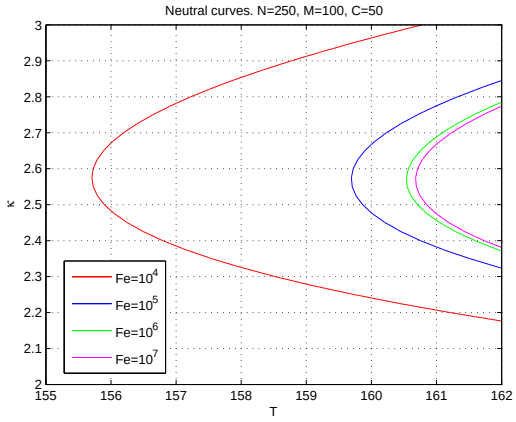

Figure 2. Neutral stability curves for electroconvection without cross-flow. Effect of charge diffusion coefficient Fe on the critical Taylor number T and disturbance wavenumber κ. Calculations with $N = 250$ Chebyshev polynomials, and $M = 100$ and $C = 50$.

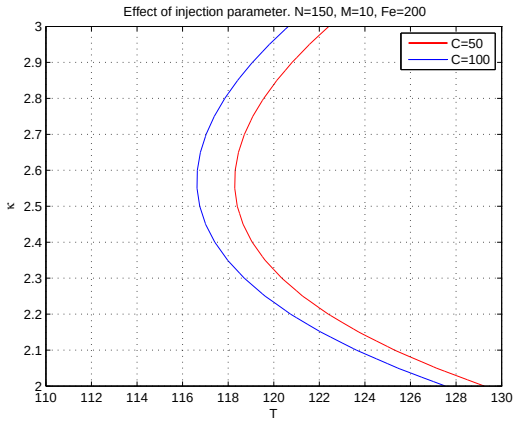

Figure 3. Neutral stability curve for electroconvection without cross-flow. Effect of injection strength coefficient C on the critical Taylor number T and disturbance wavenumber κ. Calculations with $N = 150$ Chebyshev polynomials, and $M = 10$ and $Fe = 200$.

The value of T_{cr} appears to also depend on the injection strength, though rather weakly. Figure 3 displays the neutral curves for two values of C, showing that increased injection strength produces a destabilizing effect. This is consistent with the observation that the charge density, decreasing from injector to collector, creates a potentially unstable situation, where a charge moving towards the collector will experience an increase in Coulomb force which acts to increase such movement. This results casts some doubt on the general belief that, in the so-called strong injection regime, $C \gg 1$, the value of T_{cr} does not depend on C. Lastly, we have verified that the value of M has no effect on determining T_{cr}; this is analogous to the role of the Prandtl number in Rayleigh-Bénard convection.

Given the strong sensitivity of T_{cr} to the value of Fe, we

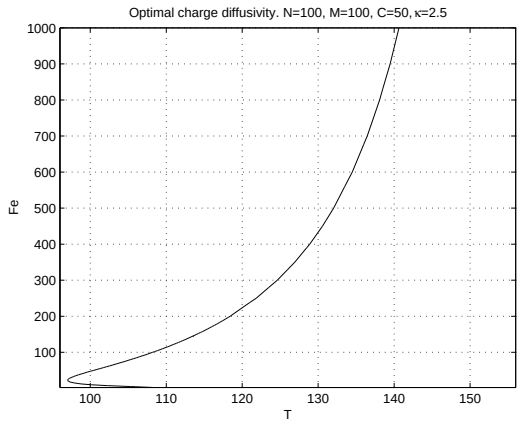

Figure 4. Change of the critical value of the Taylor number T_{cr} with Fe, for $N = 100$, $M = 100$ and $\kappa = 2.5$.

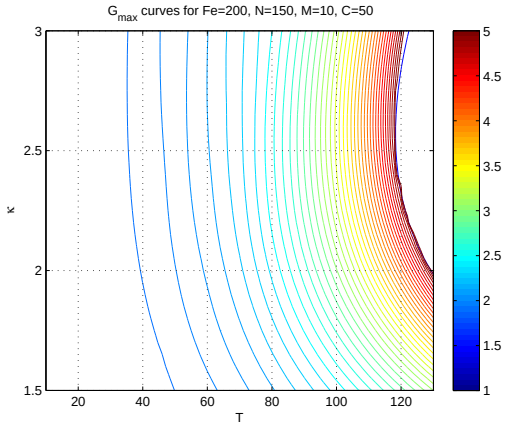

Figure 5. Maximum transient growth of perturbation energy computed for $N = 150$, $M = 10$, $C = 50$ and $Fe = 200$. The white region in the top-right corner is the one of asymptotic instability.

report in figure 4 the results of the search for the "optimal" diffusivity, i.e. for the value of Fe that yields the lowest T_{cr}. This search is performed for $\kappa = 2.5$ which approximately identifies the most unstable perturbation (see figure 2 and 3). It is observed that, at low values of Fe which are representative of dielectric fluids used in applications, T_{cr} may differ significantly from the predicted $T_{cr} = 161$ of previous numerical studies neglecting diffusion; experiments, on the other hand, report a value of $T_{cr} \approx 100$.

Non-modal stability

Non-modal stability is unexplored to date for the electroconvection problem, even in absence of cross-flow. We thus want to ascertain whether this flow supports a transient growth mechanism. This is shown to be the case in figure 5 where modest transient growth is observed, with a maximally 5-fold increase of perturbation energy in the proximity of the neutral curve. Below $T = 35$ the energy of the initial condition decays monotonically towards zero. (Due to space constraints, optimal disturbances, i.e. initial conditions leading to maximum energy amplifications, will only be discussed for the case of cross-flow; see below).

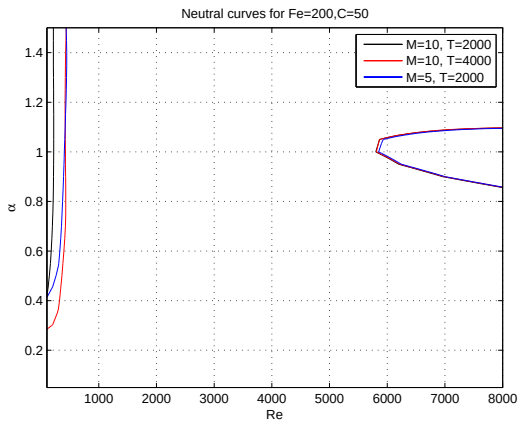

Figure 6. Neutral stability curves for $N = 150$, $C = 50$ and $Fe = 200$. At $Re = 0$ the previous analysis without cross-flow is recovered.

THE CASE WITH CROSS-FLOW

When a Poiseuille cross-flow is added, the x (streamwise) and z (spanwise) directions change character. The stability analysis of the previous section becomes two-dimensional, where the streamwise and spanwise wavenumbers α and β of the perturbations play distinct roles.

Modal stability

Traditional asymptotic stability analysis of standard Poiseuille flow starts with the fact that the modes of the normal vorticity equation, i.e. the Squire modes, are always damped, so that the entire system becomes first unstable to perturbations with $\beta = 0$. Similar arguments can be used in our case and lead to the conclusion that two-dimensional perturbations are the first to become unstable. In figure 6, on the top right, one observes the usual neutral curve for the Orr-Sommerfeld problem, where the electrical parameter do not appear to play a significant role, and the known critical value $Re_{cr} = 5773$ is obtained. On the left, the instability region determined by electroconvection is confined to very low values of Re. In this region, we have agreement with the main results of our previous analysis of EHD without cross-flow, which exactly corresponds to $Re = 0$. There is also qualitative agreement with the approximate results presented by Castellanos & Agrait (1992), who suggested that at low Re the cross-flow acts to weaken the EHD instability, while at higher Re the effects of electrical disturbances tend to be overcome by those of the velocity perturbations.

The different nature of the instability at lower and higher Re can be easily appreciated by looking at the spatial shape of the unstable modes. Figure 7 shows a portion of the entire spectrum of the system matrix, with the red circle marking the most unstable mode, which is an electric one. Its spatial shape is described by the wall-normal distribution of its

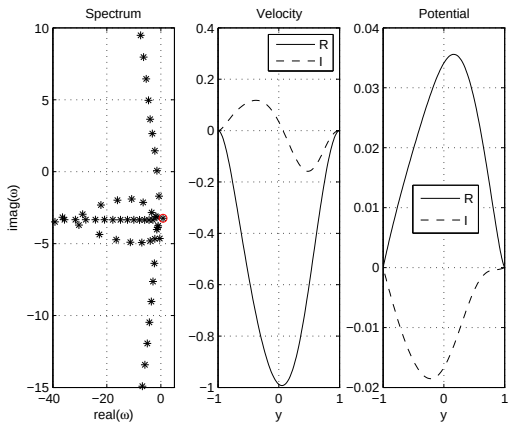

Figure 7. Discrete spectrum and spatial shape of the most unstable mode at $Re = 100$ and $\alpha = 1$ (electric mode, highlighted by the red circle).

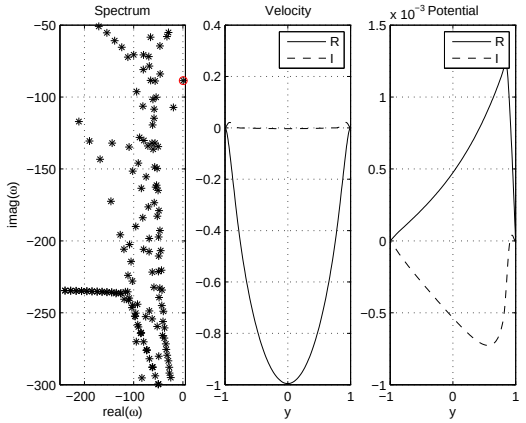

Figure 8. Discrete spectrum and spatial shape of the most unstable mode at $Re = 7000$ and $\alpha = 1$ (Poiseuille mode, highlighted by the red circle).

amplitude, in terms of vertical velocity and electric potential (wall-normal vorticity is null for $\beta = 0$). It is worth noting that the unstable mode, and in particular its electric part, is not symmetric with respect to the centerline. Increasing Re up to $Re = 7000$ (at constant α) we obtain a different picture, shown in figure 8, where the most unstable eigenvalue coincides with one of the usual spectral branches of the standard Orr–Sommerfeld, its spatial form is consistent with a Tollmien-Schlichting wave. It can be further observed that for $\alpha = 0$ the equations simplify, with the parabolic base flow vanishing from the $\hat{v}$ and $\hat{\psi}$ equations. With the Squire modes always stable, the stability properties in this case hence reduce to those of the hydrostatic case.

Non-modal stability

Transient growth is considered first in figure 9 for two-dimensional perturbations with $\beta = 0$. For $Re < 5773$, the maximum values G_{max} for transient growth are larger than those for the standard Orr-Sommerfeld case (denoted

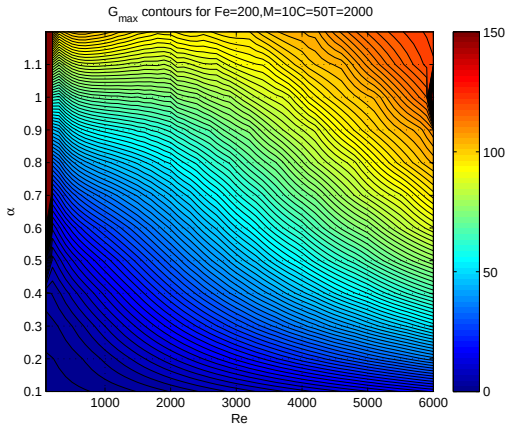

Figure 9. Maximum transient growth of perturbation energy $G_{max}(\alpha, 0, Re)$ computed for $N = 150$, $M = 10$, $C = 50$ and $Fe = 200$ and $T = 2000$.

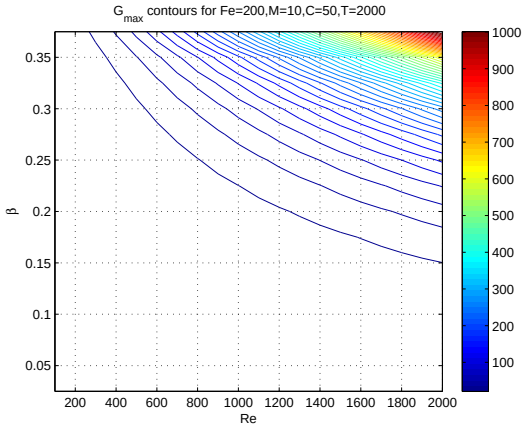

Figure 10. Maximum transient growth of perturbation energy $G_{max}(0, \beta, Re)$ computed for $N = 150$, $M = 10$, $C = 50$ and $Fe = 200$ and $T = 2000$.

$G_{max,OS}$). For example, at $Re = 5000$ and $\alpha = 1$, we have $G_{max} \approx 125$ compared to $G_{max,OS} \approx 30$ for the pure Poiseuille case.

A similar observation can be reported for the streamwise-constant perturbations, $\alpha = 0$. Figure 10 confirms the presence of strong transient growth; for example at $Re = 1000$ and $\beta = 0.35$ we have $G_{max} \approx 300$ while $G_{max,OS} \approx 10$. It can be further observed that in the governing equations, once adapted to the case $\alpha = 0$, the cross-flow $\overline{U}$ is always multiplied by α and thus vanishes for the case $\alpha = 0$.

It is interesting and instructive to determine the shape of the optimal initial condition in physical space and observe how this initial condition evolves in time to yield the maximum amplification of energy. For spanwise-independent perturbations, figures 11 and 12 highlight that the transient growth is due to an Orr-type mechanism, which describes short-term instabilities based on the tilting of initial disturbances, originally opposing the mean shear, into its direction. Moreover, the non-symmetric EHD problem produces

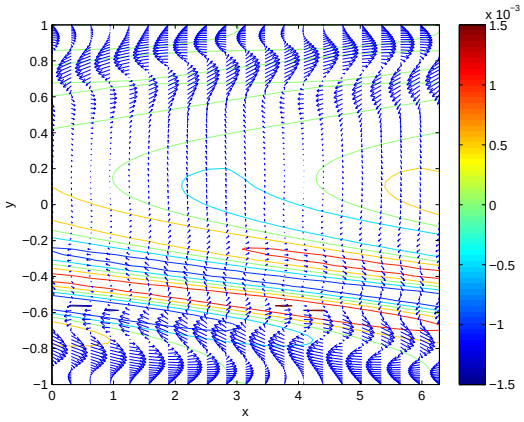

Figure 11. Optimal initial condition for $Re = 1000$, $\alpha = 1$ and $\beta = 0$ (Orr mechanism), in the $x-y$ plane. Arrows denote the in-plane velocity field, and contour lines (color band) represent the field of perturbation potential ψ.

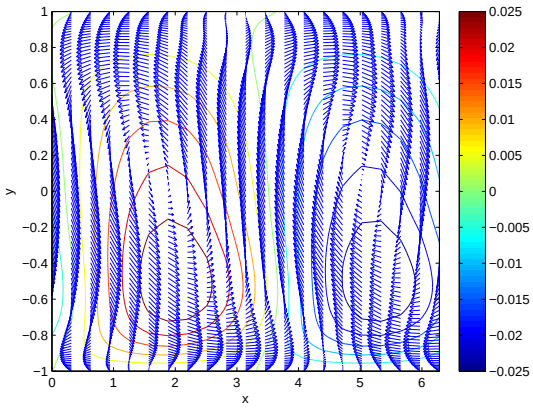

Figure 12. Optimal state at $t = t_{G_{max}}$ for $Re = 1000$, $\alpha = 1$ and $\beta = 0$ (Orr mechanism).

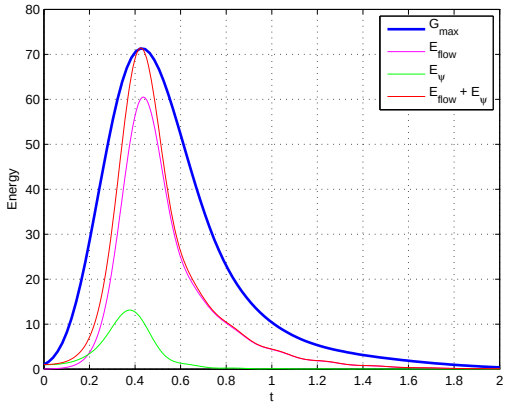

Figure 13. Disturbance energy for $Re = 1000$, $\alpha = 1$ and $\beta = 0$ (Orr mechanism).

an initial condition which is clearly non-symmetric with respect to the channel center-line. Figure 13, besides verifying that these initial conditions in fact produce the expected total energy growth and at the expected time, allows us to isolate the two contributions in form of the kinetic and electric energy; the latter is dominant, but at relevant times the electric contribution is far from negligible, and reaches is maximum quite sooner than the total energy.

For $\alpha = 0$, on the other hand, the mechanism at work is found to be a lift-up mechanism, where horizontal velocity perturbations are generated by the vertical lift-up of fluid elements in the presence of mean shear.

Conclusions

In this work we have evaluated the complete linear stability characteristics of a flow bounded by two plane walls and driven by electroconvective motion and/or pressure-gradient cross-flow. The long-term stability was already described in the literature; here we suggest that finite values of charge diffusion, previously neglected, could help explaining the discrepancy between the critical value of the forcing parameters measured in experiments and computed by numerical studies. A finite-time analysis has then shown the flow to present transient-growth phenomena, although in absolute terms this effect is not particularly strong, with a maximum amplification of energy of about 5.

We have then addressed the more complex flow induced by electroconvection in presence of a laminar Poiseuille cross-flow. For this case too, modal and non-modal analyses have been carried out. The result of asymptotic stability tells us that the EHD instability is dominant at very low *Re*, but at higher *Re* is weakened by the cross-flow. Perhaps the most interesting result comes from the non-modal analysis of the case with cross-flow. Our preliminary analysis seems to hint at a mechanism responsible for a rather strong short-time instability. In other words, the electroconvection-induced flow interacts with the instability mechanisms naturally present in the Poiseuille case to increase by orders-of-magnitude the short-time energy growth of perturbations.

REFERENCES

Atten, P. 1996 Electrohydrodynamic instability and motion induced by injected space charge in insulating liquids. *IEEE Trans. Diel. Electr. Ins.* **3** (1), 1.

Castellanos, A. 1991 Coulomb-driven convection in electrohydrodynamics. *IEEE Trans. Electrical Insulation* **26** (6), 1201–1215.

Castellanos, A. & Agrait, N. 1992 Unipolar injection induced instabilities in plane parallel flows. *IEEE Trans. Industrial Applications* **28** (3), 513–519.

Crowley, J.M. 1986 *Fundamentals of Applied Electrostatics*. Wiley, New York.

Felici, N.J. 1971 *Conduction in Liquid Dielectrics (Part II) Electrohydrodynamic Phenomena, Direct Current*, , vol. 2.

Schmid, P.J. & Henningson, D.S. 2001 *Stability and Transition in Shear Flows*. Springer.

Schoppa, W. & Hussain, F. 1998 A large-scale control strategy for drag reduction in turbulent boundary layers. *Phys. Fluids* **10** (5), 1049–1051.